ASD-TDR-62-479
Part I

RESEARCH AND DEVELOPMENT ON THE EFFECTS OF HIGH PRESSURE ON VARIOUS ELEMENTS AND BINARY ALLOYS

Part I. Effect of Pressure on the Austenite to Pearlite Reaction

TECHNICAL DOCUMENTARY REPORT NO. ASD-TDR-62-479, PART I

May 1963

Directorate of Materials and Processes
(Materials Central)
Aeronautical Systems Division
Air Force Systems Command
Wright-Patterson Air Force Base, Ohio

Project No. 7351, Task No. 735103

(Prepared under Contract No. AF-33(616)-8206 by General Electric Co., Schenectady, New York; J. E. Hilliard, Author)

NOTICES

When Government drawings, specifications, or other data are used for any purpose other than in connection with a definitely related Government procurement operation, the United States Government thereby incurs no responsibility nor any obligation whatsoever; and the fact that the Government may have formulated, furnished, or in any way supplied the said drawings, specifications, or other data is not to be regarded by implication or otherwise as in any manner licensing the holder or any other person or corporation, or conveying any rights or permission to manufacture, use, or sell any patented invention that may in any way be related thereto.

Qualified requesters may obtain copies of this report from the Armed Services Technical Information Agency (ASTIA), Arlington Hall Station, Arlington 12, Virginia.

This report has been released to the Office of Technical Services, U. S. Department of Commerce, Washington 25, D. C., in stock quantities for sale to the general public.

Copies of this report should not be returned to the Aeronautical Systems Division unless return is required by security considerations, contractural obligations, or notice on a specific document.

34-837C, 700, 6-28-63

FOREWORD

The report was prepared by the General Electric Research Laboratory, General Electric Company, Schenectady, New York under Contract No. AF 33(616)-8206. This contract was initiated under Project No. 7351, "Metallic Materials," Task No. 735103, "Unique Metallic Materials and Techniques." The work was administered under the direction of the Directorate of Materials and Processes (Materials Central), Deputy for Technology, Aeronautical Systems Division, with Mr. K.L. Kojola acting as project engineer.

This report covers work conducted from 1 April 1961 to 1 April 1962. Part I of the report describes an investigation made by J.E. Hilliard on the effect of pressure on the austenite-pearlite reaction.

Additional work was performed by W.F. Claussen on the effect of pressure on transformations in iron and iron alloys. This work is presented separately as Part II of the report.

The author is indebted to the following members of the General Electric Research Laboratory for their assistance in this investigation: G. Dinsmore (machining of high-pressure cell assemblies); W.F. Moore (preparation of alloys); E.W. Balis (chemical analysis); T.V. Brassard (macrograph, Fig. 11); E.F. Koch (electron microscopy); J. Wilson (cell assembly); and E. Nagy (atmospheric-pressure heat treatments).

ABSTRACT

The growth rate and interlamellar spacing of pearlite have been determined as a function of transformation temperature at one atmosphere and 30 kilobars pressure in eutectoid iron-carbon alloys containing approximately one per cent manganese. The atmospheric-pressure growth rates, measured at four temperatures in the range 560° to 680°C, were in fair agreement with data obtained on a similar alloy by other investigators. Indications were found of a change in slope of the reciprocal spacing vs temperature curve at one atmosphere corresponding to the onset of partitioning of manganese between ferrite and cementite at 640°C.

High-pressure runs were made at seven temperatures in the range 400° to 620°C. In comparison with the properties of the transformation at one atmosphere, the specimens transformed at 30 kb exhibited the following changes: (a) Decrease in pearlite growth rates by factors of up to a thousand. (b) Surface nucleation of pearlite was dominant over the whole temperature range studied. (c) The surface-nucleated pearlite had a higher growth rate than the nodular pearlite nucleated in the interior. (d) There was a substantial increase in the interlamellar spacing of the pearlite. Below 580°C the average spacing (defined in terms of the ferrite-cementite boundary area) remained approximately independent of temperature. (e) The nose of the growth rate vs temperature curve was depressed by 20°, from 580° to 560°C. The maximum growth rate at 30 kb was 200 to 400 times less than the maximum rate at one atmosphere. (f) Austenitization under pressure gave no change in austenitic grain size within the standard deviation (0.1 ASTM unit) of the measurement.

The results for the effect of pressure on pearlite growth rate and spacing confirm those obtained at a single temperature in a preliminary survey made earlier in this Laboratory.

This technical documentary report has been reviewed and is approved.

I. Perlmutter

I. PERLMUTTER
Chief, Physical Metallurgy Branch
Metals and Ceramics Division
Air Force Materials Laboratory

TABLE OF CONTENTS

LIST OF FIGURES

LIST OF FIGURES (CONT'D)

LIST OF FIGURES (CONT'D)

LIST OF TABLES

INTRODUCTION

In an experimental survey[1, 2] made in this Laboratory in 1959 on the effect of pressure on the kinetics of various phase transformations, the author found a very large decrease (about 700-fold) in the growth rate of pearlite in a commercial 1080 steel at 600°C when transformed under a pressure of 32 kilobars. It was also observed that the pressure dependence of the pearlite growth rate was much smaller in a high-purity iron-carbon alloy; there being only about a five-fold decrease under the same conditions. This difference in behavior was attributed to the presence of manganese (about one per cent) in the commercial steel.

It was apparent that a full investigation of the effect of pressure on the pearlite transformation would provide a better understanding of the nature of this transformation at atmospheric pressure and, in particular, on the role played by manganese in increasing the hardenability of steel. However, it was also evident that before such an investigation would be meaningful, data would be required on the effect of pressure on certain other properties of iron-carbon alloys, the most important being the phase equilibria and the diffusion of carbon in austenite. A study of these two effects was therefore made as a preliminary to the present investigation. The results, which have been described in detail in earlier report,[3] may be summarized as follows. The application of pressure decreases the solubility of carbon in austenite and also depresses the eutectoid temperature. As a result, the eutectoid composition is displaced to a lower carbon content. A comparison of the phase boundaries at atmospheric pressure and 30 kb is shown in Fig. 1. With respect to the diffusion of carbon in austenite, the diffusivity was found to decrease with increasing pressure. The observed activation volume [given by $- RT(\partial \ln D/\partial P)_T$] is about 1 cm^3. This decrease accounts[2] quantitatively for the variation with pressure of the pearlite growth rate in a high-purity iron-carbon alloy if the assumption is made that the volume diffusion of carbon is the rate-controlling step in pearlite growth. However, it does not account for the larger pressure dependence of the growth rate in the commercial steel.

The purpose of the investigation described in this part of the report was to establish the effect of pressure on the growth rate and spacing of pearlite in a manganese steel over a range of temperature. A steel containing approximately one per cent manganese was selected for study since an extensive investigation of the pearlite transformation at atmospheric pressure has recently been made

---

Manuscript released by author July 1962 for publication as an ASD Technical Documentary Report.

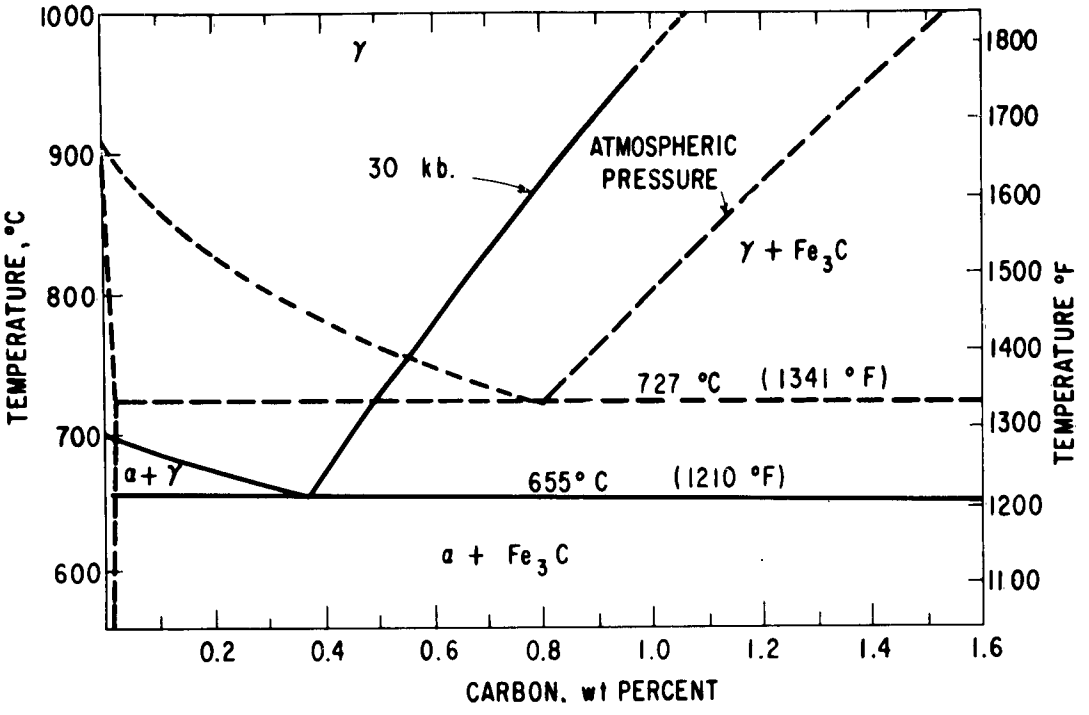

Fig. 1 A comparison between the positions of the boundaries of the iron-carbon system at atmospheric pressure and 30 kb.

for this composition by Picklesimer, McElroy, Kegley, Stansbury, and Frye.[4] Atmospheric pressure measurements were also made in the present investigation in order to determine if the transformation characteristics of the alloys were similar to those used by the latter authors. It was also necessary to determine the interlamellar pearlite spacing at atmospheric pressure since there were no suitable existing data.

EXPERIMENTAL PROCEDURE

Preparation of Alloys

Two alloys were used in this investigation: one having the nominal composition 0.75 per cent carbon and 1.00 per cent manganese which was the same as one of the alloys used by Picklesimer et al.[4] and corresponded to the eutectoid composition at atmospheric pressure; the other alloy had the nominal composition 0.35 per cent carbon and 1.00 per cent manganese corresponding[3] to the eutectoid at 30 kb.

The alloys, prepared from "Ferrovac" iron and high-purity graphite and manganese, were induction-melted in magnesia crucibles under argon. The ingots were hot-worked and swaged to 0.375-inch-diameter rods. After a homogenization anneal for 6 hours at 1250°C under vacuum, samples were removed from each end of the rods for chemical analysis. The results of the analyses are given in Table I; for comparison, the analysis of "steel A" used by Picklesimer et al.[4] is also included. It can be seen that alloy X closely approaches "steel A" in composition.

TABLE I

Chemical Analyses of Iron Alloys

Element	Present Investigation		Picklesimer et al.[4]
	Alloy W	Alloy X	Steel A
Carbon	0.33	0.73	0.75
Manganese	1.00	.97	1.02
Silicon	<0.005	.01	0.03
Phosphorus	.003	.003	.003
Sulfur	.01	.01	.013

For the atmospheric-pressure studies, the 0.375-inch-diameter rods were cut into disks 0.125-inch thick with a hole 0.03-inch diameter drilled through the center so that they could be hung from wires for the isothermal heat treatments. The disks were copper-plated to retard decarburization.

The specimens for the high-pressure anneals were in the form of pills 0.125-inch diameter by 0.06-inch thick. These were prepared from rods which had been swaged to 0.19 inch and then centerless ground to 0.125-inch diameter. The pills were plated with silver to reduce decarburization. Silver is preferable to copper for this purpose because of its very low solubility for carbon and its mutual immiscibility with iron. However, it could not be used on the atmospheric-pressure specimens because of its low melting point. This factor did not apply in the case of the high-pressure specimens because, at the pressure of 30 kb, the melting point of silver is raised above the temperature of 1050°C used for austenitization.

Atmospheric-Pressure Heat Treatments

Isothermal transformations at atmospheric pressure were made at four temperatures in the range 560° to 680°C. The heat treatments were carried out in salt pots containing "Houghton's Liquid Ht 1550." All specimens were austenitized for 10 minutes at 1050°C and then transferred as rapidly as possible to the second

pot at the transformation temperature. After holding for the required time, the specimens were quenched in water. The specimen disks were sectioned across a diameter for optical and electron microscopy.

High-Pressure Heat Treatments

The high-pressure runs were carried out in the "belt" apparatus.(5) As shown in Fig. 2, this consisted of a cylindrical cell compressed between two Carboloy punches loaded by a uniaxle press. Radial support to the cell was given by the "belt" which was a Carboloy die heavily pre-stressed by a series of steel binding rings. Laminated gaskets of lava and metal separated the punches from the inner surface of the "belt."

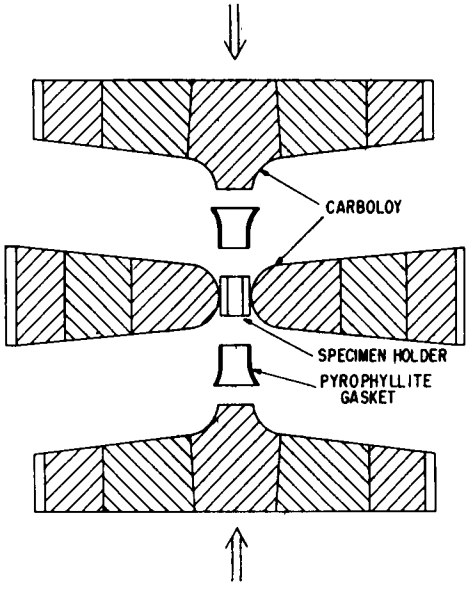

Fig. 2 "Belt" apparatus used for high-pressure heat treatments.

A cross-section of the high-pressure cell is shown in Fig. 3. Two specimen pills were located inside a resistance heater of 0.20-inch-diameter Nichrome tubing. The ends of the tube were sealed with alumina and lava pills tamped in place after the space around the specimens had been filled with sodium chloride. The plasticity of the latter reduced the degree of nonhydrostatic loading on the specimens. However, any solid pressure-transmitting medium introduces some nonhydrostatic deformation. It has been shown(3, 6) that completely hydrostatic conditions can be attained by encapsulating the specimens with a fluid. However, this precaution was considered unnecessary in the present investigation

Electrical contact between the Nichrome tube and punches was made through a ring and nickel disk (not shown in figure) at each end of the cell. The

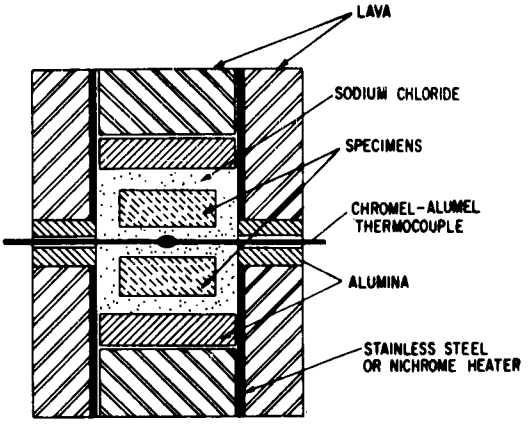

Fig. 3 High-pressure cell.

specimens could thus be heated by applying a low voltage across the two punches (which were electrically insulated from the platens of the press). The nickel disks not only provided electrical contact, but also furnished extra resistance heating to compensate for end losses.

The specimen temperature was measured by a chromel-alumel thermocouple the hot junction of which was sandwiched between the two specimens at the center of the cell (Fig. 3). The thermocouple leads were insulated and brought out between the gasket and the "belt." All thermocouples were prepared from the same batch of wire. Samples taken from each end of this batch were calibrated at the General Engineering Laboratory of the General Electric Company. Although there was a significant deviation of the emf-temperature relationship from that given in the National Bureau of Standards tables, there was no detectable difference between samples from the two ends of the batch. The thermal emf was measured with a potentiometer which had been calibrated against a standard instrument.

It is known that the emf of a thermocouple varies to some extent with pressure. Data[7] available at present indicate that the pressure dependence is much smaller for chromel-alumel than it is for platinum/platinum-rhodium thermocouples. However, the absolute magnitude of the effect is still uncertain for the pressure-temperature range covered by the present investigation. The conversion from thermal emf to temperature was therefore made on the basis of the atmospheric-pressure calibration with no correction for the pressure dependence. Consequently, the temperatures cited in this report are subject to revision when further thermal emf data become available. It is anticipated, however, that the necessary correction will not exceed a few degrees.

During the high-pressure runs the temperature was controlled by applying the out-of-balance thermal emf to a null-detecting instrument, which actuated a motor-driven Variac on the input to the power supply of the heater. This system in conjunction with stabilization of the power supply permitted the thermocouple reading to be held constant within $\pm$ 1°C for an indefinite period.

The oil pressure on the ram of the press was measured with a 0 to 3000 psi Heise gage. The relationship between the oil pressure and the pressure inside the cell was determined[8] by observations of the bismuth I→ II transition at 25.3 kb and the transition in barium at 59 kb. The transitions were detected by electrical resistance measurements using the cell shown in Fig. 4. In the vicinity of the transitions, the oil pressure was increased in increments corresponding to 0.2 kb. For bismuth, the onset of the transition was well defined and reproducible to within this pressure interval. The barium transition was appreciably less sharp, and there was a correspondingly greater uncertainty in defining its pressure. The calibration runs were repeated whenever dimensional changes in the dies indicated it to be necessary. Pressures between 25.3 and 59 kb were estimated by linear interpolation.

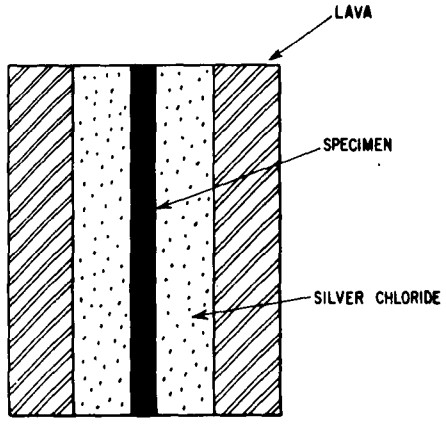

Fig. 4 High-pressure cell used for calibration of the "belt" apparatus.

The pressure-temperature cycle used in heat treatment of alloy W is shown in Fig. 5. All runs were made at 30 kb and the specimens were austenitized under pressure for 10 minutes at 1050°C. The temperature was then decreased as rapidly as possible to the transformation temperature. After holding for times ranging from 1 to 60 minutes, the specimens were rapidly cooled to room temperature under pressure by switching off the power to the heater. Because of the large thermal mass surrounding the cell, the cooling rate exceeded 200°C per second, which was sufficient to act as a "quench."

After removal from the cell, the specimens were mounted in bakelite and sectioned for metallographic examination on a diametrical plane parallel to the short axis.

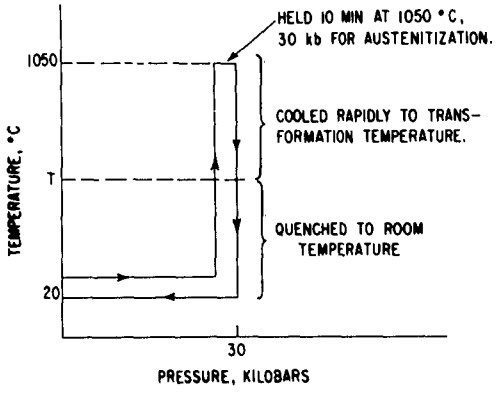

Fig. 5 Pressure-temperature cycle used for heat treatments. For clarity, the two halves of the cycle are shown displaced from one another, but in practice they were coincident.

EXPERIMENTAL RESULTS

Specimens were transformed isothermally at a series of temperatures at both atmospheric pressure and 30 kb. Measurements were made of: pearlite growth rate and interlamellar spacing, austenitic grain size, and volume fraction transformed. The last measurement was made only on the specimens transformed at atmospheric pressure.

Pearlite Growth Rate

In some of the atmospheric-pressure specimens there was a slight tendency for preferential nucleation of pearlite at a free surface. The opposite effect (a lower density of nodules in the vicinity of the surface) was also seen occasionally. Neither of these two effects varied in a systematic manner with the transformation temperature, contrary to the usual observation that high temperatures favor surface nucleation. One curious phenomenon observed in the present study was the preferential nucleation of pearlite at cracks formed during the quench from the austenitizing temperature. An example is shown in Fig. 6 in which it will be noted that there was a copious growth of pearlite around the crack but none at the surface. There are two reasons for believing that the crack was the cause and not the result of the pearlite growth; one was the fact that cracks free of pearlite were seen in the specimen, and the other was the absence of continuity in the structure of the pearlite across the crack. A possible explanation of the phenomenon is that a freshly formed surface offers a more potent nucleation site than does a surface contaminated by oxides and heat-treating salt.

The procedure used for estimating the pearlite growth rate in the specimens transformed at atmospheric pressure was the usual one of measuring the maximum nodule radius in a series of specimens transformed for different times at the same temperature. A slope of the plot of maximum nodule radius vs time is then taken as the growth rate at that temperature. This procedure is based on the assumption that the nodules are spherical or hemispherical, and that the maximum radius seen on the plane of polish is equal to the radius of the largest nodule present in the specimen. The measurement is therefore simple enough in principle but not, unfortunately, in practice. In the first place, many of the samples in the present investigation displayed nodules that were not even approximately spherical or hemispherical. An example from one of the pressure runs is shown in Fig. 7. In such cases there was an ambiguity as to what measurement would correspond to a "maximum radius." A second difficulty arises from impingement of nodules. This factor set an upper limit to the transformation time at which meaningful measurements could be made. And, although the probability of impingement decreases rapidly with decreasing volume fraction of pearlite, the probability is never zero. Consequently, even at the smallest volume fractions, the largest "nodule" will always in fact be a cluster of two or more individual nodules if the search is continued long enough. The occurrence of irregular-shaped nodules and the necessity of excluding those which might have impinged introduced a strong subjective element into the measurements. Apart from these difficulties, it must also be noted that measurements of nodule radii yield an estimate of only the maximum growth rate.

Fig. 6 Run 33. Example of preferential nucleation of pearlite at crack in specimen transformed 15.5 sec at 639°C at atmospheric pressure. Nital etch. 200X

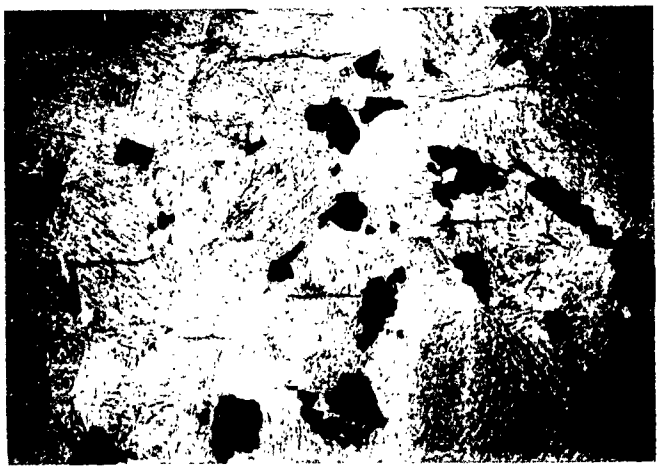

Fig. 7 Run 136. Alloy W transformed for 5 min at 480°C and 30 kb. Nital etch. 200X

The nodule radii were measured directly under the microscope using an eyepiece with a calibrated reticule. Measurements were confined to nodules away from the surface of the specimens since, as will be shown, there was evidence that surface-nucleated pearlite does not necessarily have the same growth rate as that formed in the interior.

The results for alloy X transformed at 562°, 599°, 639°, and 680°C at atmospheric pressure are listed in Table II. Plots of maximum nodule radius vs time for these four temperatures are shown in Figs. 8 and 9. All the plots have positive intersections on the time axis indicating an apparent delay in the onset of nucleaation. The growth rates given in Table III were calculated from the

TABLE II

Pearlite Growth vs Temperature at Atmospheric Pressure in a 0.73% C, 0.97% Mn Fe Alloy

Run	Temp. (°C)	Time (sec)	Maximum Nodule Radius (10^{-3} cm)	Pearlite Volume Fraction (%)
10	562	3	0	0
11	↓	5.5	1.8	0.0033±0.001
12		7	3.5	.59 ± .10
13		8	6.2	13.7 ±1.0
14		10	10.7	66.1 ±3.5
15		16.5	-	~100
16		32.5	-	100
17	↓	64.5	-	100
20	599	1	0	0
21	↓	2	0	0
22		4.5	0	0
23		6	1.3	0
24		7.5	2.9	0.058 ±0.01
25		10.5	5.4	4.8 ± .5
26	↓	18	-	99.5 ± .2
27		32	-	~100
30	639	3	0	0
31	↓	6	0	0
32		11	0	0
33		15.5	2.1	0.018 ±0.006
34		22.5	7.0	1.5 ± .3
35		29	13.5	17.8 ±2.0
36		36	-	62.8 ±3.6
37		49.5	-	93.3 ±1.2
38	↓	96 (min)	-	100
40	680	7	-	-
41	↓	12	5.6	-
42		20	12.1	-
43		40	-	-
44		80	-	-
45	↓	160	-	-

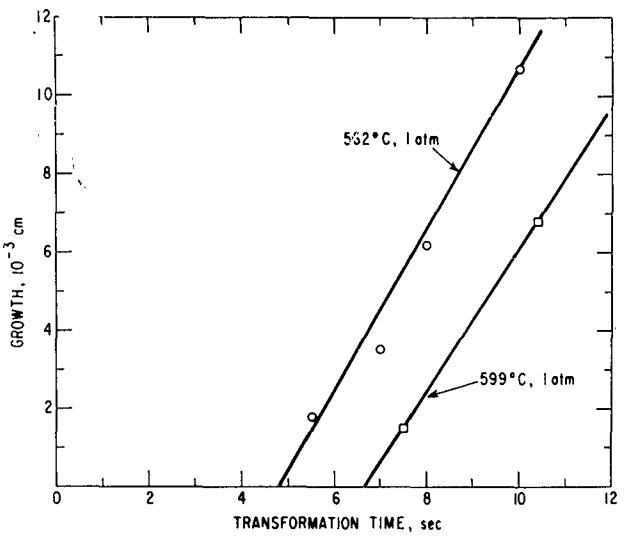

Fig. 8 Maximum nodule radius vs time for alloy X transformed at 562° and 599°C at atmospheric pressure after austenitization for 10 min at 1050°C.

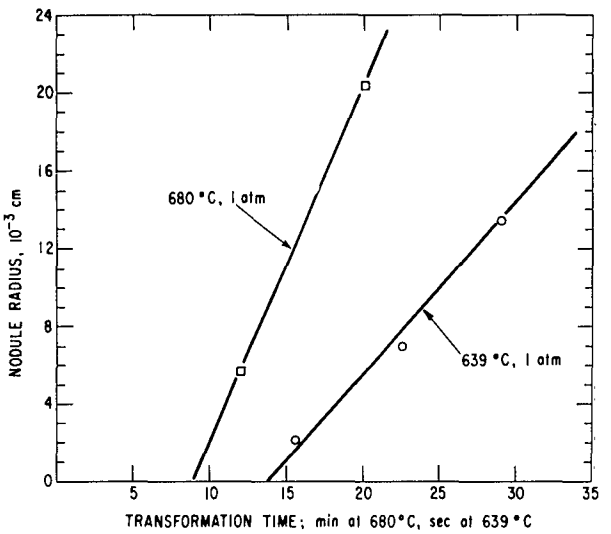

Fig. 9 Maximum nodule radius vs time for alloy X transformed at 639° and 680°C at atmospheric pressure after austenitization for 10 min at 1050°C.

slope of the plots in Figs. 8 and 9 and are plotted vs temperature in Fig. 10. The data obtained by Picklesimer et al. (4) on "steel A" are included for comparison in both the table and the figure. It will be noted that the growth rates observed in the present investigation displayed a similar temperature variation but were consistently lower than those reported on a similar alloy by Picklesimer et al. This difference may be indicative of a slight variation in the behavior of the two alloys, but it could also have arisen from experimental errors together with the uncertainty introduced by the subjective nature of the measurements. Of the two

TABLE III

Pearlite Growth Rate vs Temperature
at Atmospheric Pressure

Temperature (°C)	Growth Rate (10^{-3} cm sec^{-1})	
	This Investigation*	Picklesimer et al.[4]†
562	2.1	2.6
599	1.8	2.6
639	0.91	1.3
680	.031	0.14

*0.73% carbon, 0.97% manganese alloy X.

†0.75% carbon, 1.02% manganese alloy (Steel A, Table I).

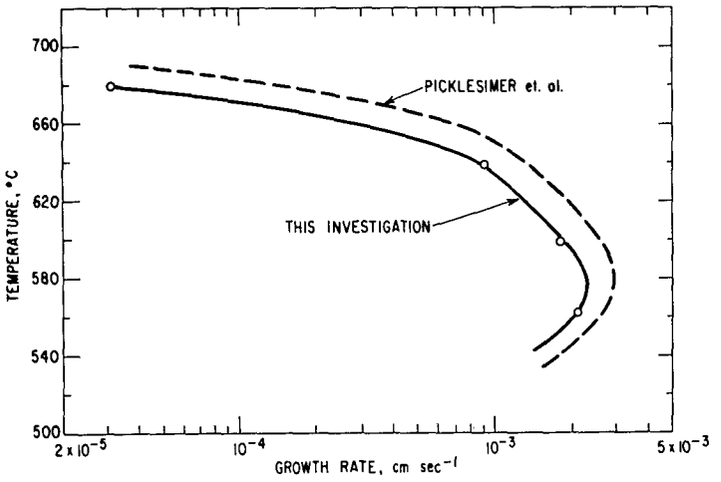

Fig. 10 Pearlite growth rate vs temperature for alloy X transformed at atmospheric pressure. Data derived from slopes of plots in Figs. 9 and 10. Curve obtained by Picklesimer et al.[4] for "Steel A" of similar composition (see Table I) is included for comparison.

sets of data, that of Picklesimer et al. is undoubtedly the more reliable because of the greater number of runs made and the superior method of transferring the specimens during heat treatment.

The high-pressure transformation studies were made on the 0.33 per cent carbon alloy W which, according to the phase-diagram investigation,[3] is the approximate eutectoid composition at 30 kb. Runs were made at this pressure at seven temperatures covering the range 440° to 620°C. (In addition, there was a 400°C run for spacing measurements only.)

A notable feature of the transformation at 30 kb was the occurrence of preferential surface nucleation of pearlite throughout the whole temperature range. All the specimens displayed (see Fig. 11, for example) a slab of pearlite around the free surfaces. This effect was not only of considerable interest in itself, but it also permitted more reliable estimates of the pearlite growth rates than were possible in the specimens transformed at atmospheric pressure. The reason for this is that, since the pearlite growth was essentially normal to the surface, the penetration observed on the plane of polish (which was also normal to the surface) gave a direct estimate of the true growth distance. Three types of measurements were therefore possible on the pressure-treated specimens: (a) Maximum growth distance from surface; this was taken as the greatest distance of penetration on either of the two specimens in each run. Maxima arising from the impingement of an interior nodule with the surface slab were excluded where detectable. (b) Average growth from surface; this was determined by taking the average of 40 to 60 measurements of penetration distance at approximately constant, but randomly selected intervals across the plane faces of the two specimens for each run. The average growth distance so obtained corresponded to the thickness of a uniform slab that would have had the same volume as the actual slab. (c) Maximum nodule radius; this was the same measurement as that made on the specimens transformed at atmospheric pressure. Data were obtainable only from runs at 560°C and below because at higher temperatures no interior nodules were nucleated even after transformation times which allowed considerable growth from the surface.

The results of these three measurements on specimens transformed at 440°, 480°, 520°, 560°, 580°, 600°, and 620°C are listed in Table IV and are plotted vs time in Figs. 12 to 18. It will be seen that within the limits of experimental error the growth as represented by all three measurements was linear with time, and that the surface growth extrapolated either to zero or a small positive quantity at time zero. The nonzero extrapolations in the 440° and 480°C plots (Figs. 12 and 13) were due to the formation of some pearlite during the cooling from the austenitization to the transformation temperature. This

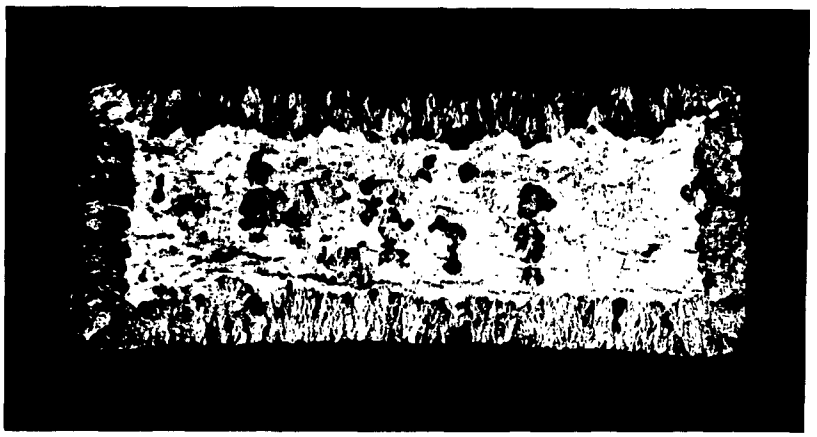

Fig. 11 Run 154. Alloy W transformed for 5 min at 560°C and 30kb. Nital etch. 35X

TABLE IV

Pearlite Growth vs Temperature at 30 kb
in a 0.33% C, 1.00% Mn Fe Alloy W

Run	Temperature (°C)	Time (min)	Pearlite Growth (10^{-3} cm)		
			Maximum Surface	Average Surface	Maximum Nodule Radius
110	400	60	-	-	-
120	440	0	1.7	0.2	0
121		1	4.1	1.8	0.6
122		3	6.3	2.6	2.2
123		3	6.4	2.9	1.6
124		6	10.7	4.0	2.9
125	⋎	60	-	-	-
130	480	0	1.1	0	0
131		1	4.8	2.5	0.9
132		2	6.4	4.2	2.4
133		3	11.8	5.9	3.8
134		4	13.4	7.9	3.8
135		5	13.4	6.6	7.0
136	⋎	5	14.5	7.3	5.4
137	478	20	-	-	-
140	520	1	5.9	3.6	0
141		2	8.0	4.9	1.9
142		2	8.6	5.7	2.1
143		3	11.8	9.5	5.9
144		3	13.4	9.3	4.3
145		4	18.2	10.0	5.4
146		5	20.4	15.3	7.0
147	⋎	15	-	-	-
150	560	1	7.5	4.5	0
151		2	11.3	7.3	0
152		3	19.3	10.0	3.2
153		4	25.2	17.2	7.5
154		5	30.6	24.8	8.6
155	⋎	15	-	-	-
160	580	2	9.6	6.0	0
161		4	14.5	6.8	0
162	⋎	6	22.0	14.2	0
170	600	5	5.4	2.8	0
171		10	8.6	4.6	0
172	⋎	15	14.5	6.0	0
173		20	16.1	9 0	0
180	620	20	2.7	1.6	0
181		40	6.4	2.7	0
182	⋎	60	8.0	4.6	0

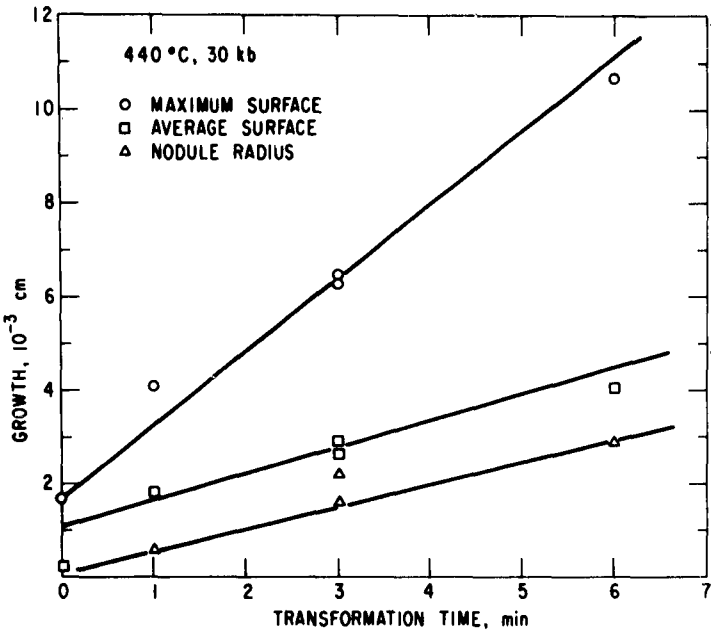

Fig. 12 Pearlite growth vs time for alloy W transformed at 440°C and 30 kb.

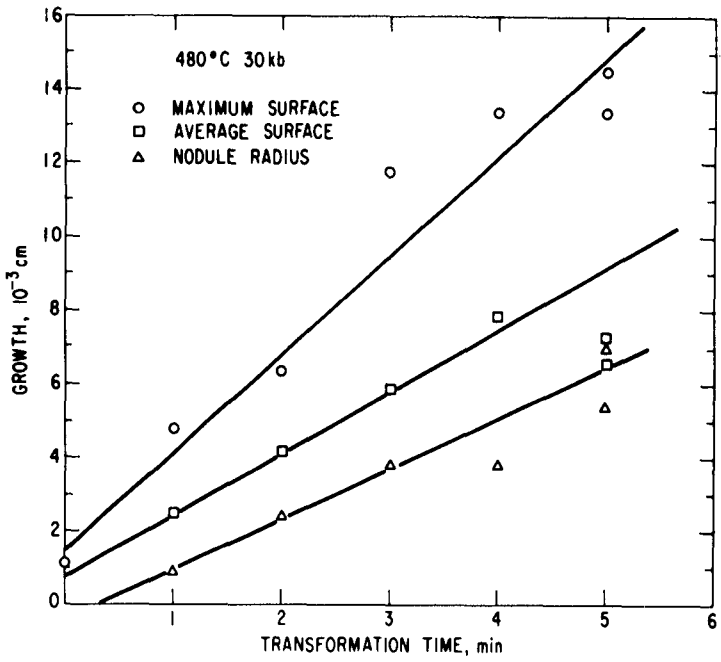

Fig. 13 Pearlite growth vs time for alloy W transformed at 480°C and 30 kb.

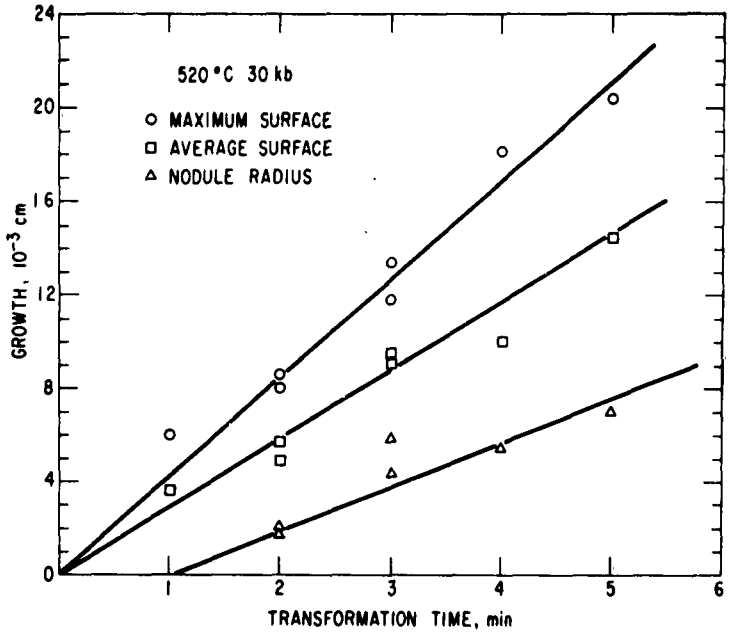

Fig. 14 Pearlite growth vs time for alloy W transformed at 520°C and 30 kb.

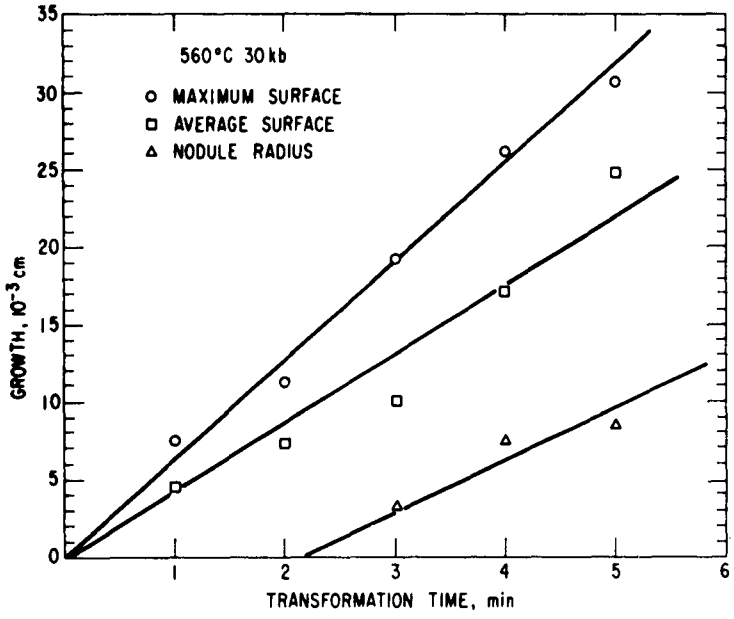

Fig. 15 Pearlite growth vs time for alloy W transformed at 560°C and 30 kb.

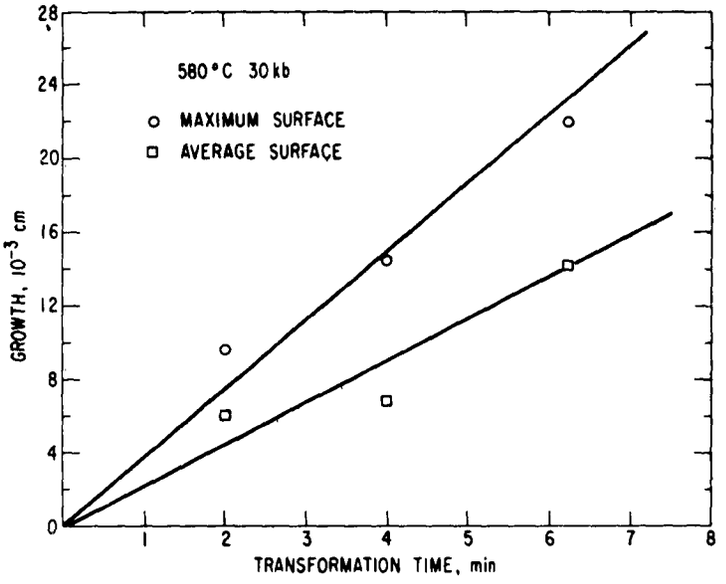

Fig. 16 Pearlite growth vs time for allow W transformed at 580°C and 30 kb.

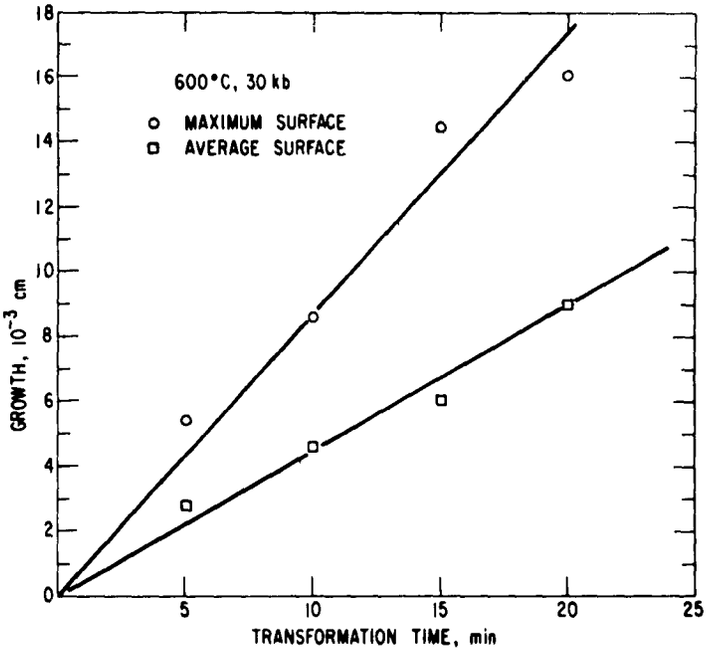

Fig. 17 Pearlite growth vs time for alloy W transformed at 600°C and 30 kb.

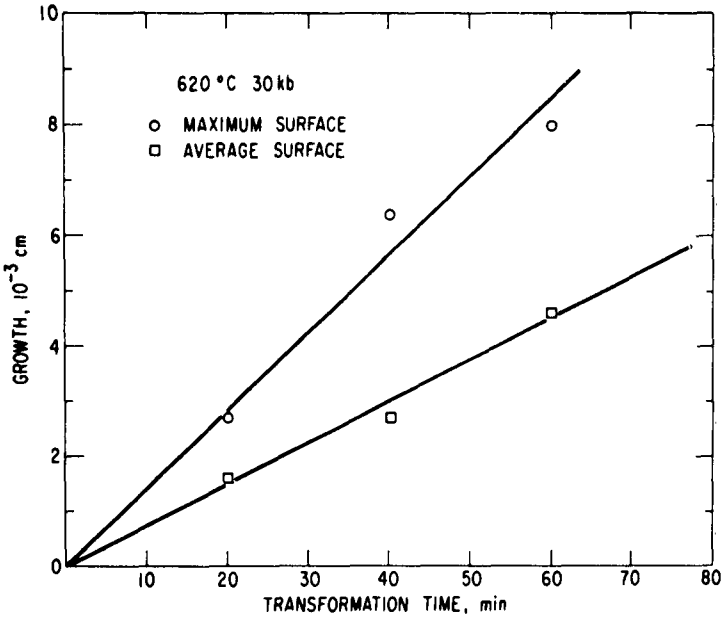

Fig. 18 Pearlite growth vs time for alloy W transformed at 620°C and 30 kb.

explanation was verified by runs 120 and 130 in which specimens were quenched immediately the transformation temperature had been reached. In both runs, as indicated in Table IV, a thin layer of pearlite was found around the surface.

From the slopes of the growth vs time plots the values listed in Table V were derived for the growth rates corresponding to the three types of measurements. These data are plotted as a function of temperature in Fig. 19 It will be seen that at mid-temperatures the maximum surface growth rate was about 1.5 times the average; this increased gradually to a factor of 1.9 at 620°C. The lowest temperature tested (440°C) exhibited a much greater difference between the two growth rates, the maximum being about three times the average. This large increase corresponded to a change in the morphology of the pearlite at the low transformation temperatures. As will be seen from a comparison of Figs. 11 and 20, the high-temperature pearlite exhibited a fairly uniform front whereas that formed at 440°C is acicular. (Some observers would term the constituent shown in Fig. 20 bainite rather than pearlite; however, as will be shown later, there was no discontinuous change in the fine structure of the transformation product in going from high to low temperatures.)

It will also be seen from Fig. 19 that, over the temperature range where measurements were possible, the growth rate given by the maximum nodule radius is consistently less than the average growth rate of the surface-nucleated pearlite. As previously noted, measurements of nodule radii yield the value of the maximum growth rate in the interior. It must therefore be concluded that pearlite nucleated at the surface grew two or three times more rapidly than that nucleated within the specimen. This is contrary to the observations of Picklesimer et al.[4] at

TABLE V

Pearlite Growth Rate vs Temperature at 30 kb
in a 0.33% C, 1.00% Mn Fe Alloy W

Temperature (°C)	Pearlite Growth Rate (10^{-5} cm sec^{-1})		
	Maximum Surface	Average Surface	Nodule
440	2.6	0.9	0.8
480	4.5	2.8	2.3
520	7.0	4.9	3.1
560	10.6	7.3	5.7
580	6.2	3.8	-
600	1.45	0.75	-
620	0.24	.13	-

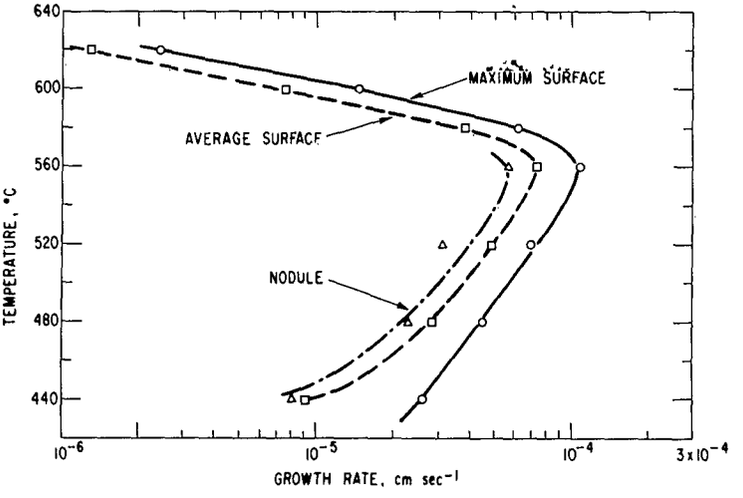

Fig. 19 Pearlite growth rate vs temperature for alloy W transformed at 30 kb. Data derived from slopes of plots in Figs. 12 to 18.

atmospheric pressure. These authors found preferential surface nucleation in their specimens transformed at 660°C and above, but measurements of the maximum growth from the surface gave the same growth rate as that for free nodules. A possible explanation for this difference between the two investigations may be an increase with pressure in the segregation ahead of the advancing pearlite-austenite interface. An indication that this effect was operative is to be found in the growth plots (Figs. 12 to 18). It will be observed that for every

temperature the point on the surface growth plots for the shortest transformation time fell above the average. For any one plot the discrepancy could be accounted for by experimental error, but its occurrence in all the plots strongly suggests that the growth rate from the surface underwent an initial decrease as segregation was established ahead of the pearlite interface. Additional evidence for this view was afforded by the observation in several specimens of a retardation in growth at the corners; an example of this is shown in Fig. 21.

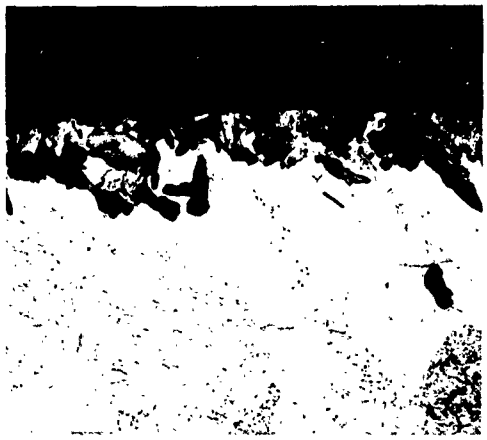

Fig. 20 Run 124. Alloy W transformed for 6 min at 440°C and 30 kb. Nital etch. 200X

Fig. 21 Run 154. Alloy W transformed for 5 min at 560°C and 30 kb. Note retarded pearlite growth at corner of specimen. Nital etch. 200X

Volume Fraction Transformed

The volume fraction of pearlite was determined for the atmospheric-pressure specimens transformed at 562°, 599°, and 639°C. No estimates were made for the runs at 680°C because some of the specimens transformed at this temperature contained pearlite formed during the quench. This additional pearlite appeared as a band (Fig. 22) around existing nodules. Because of its finer spacing it was easily detected and allowed for at the high magnifications used in measuring the nodule radii, but at the lower magnifications employed in the volume-fraction analysis the distinction could not readily be made. No measurements were made for the specimens transformed under pressure because of the predominance of the surface-nucleated pearlite.

Samples containing more than one per cent of pearlite were analyzed by a systematic point count[9, 10] using specially ruled reticules in the eyepiece of the microscope. For samples with low volume fractions, a modified point-counting procedure was employed which maximized the information obtained from a given area of the plane of polish. An experimental estimate of the standard deviation was made for all analyses.

The results together with their standard deviations are listed in the fifth column of Table II.

It can be shown[11] that the over-all rate of the pearlite transformation can be represented by an equation of the form

$$V_V = 1 - e^{-bt^n} , \qquad (1)$$

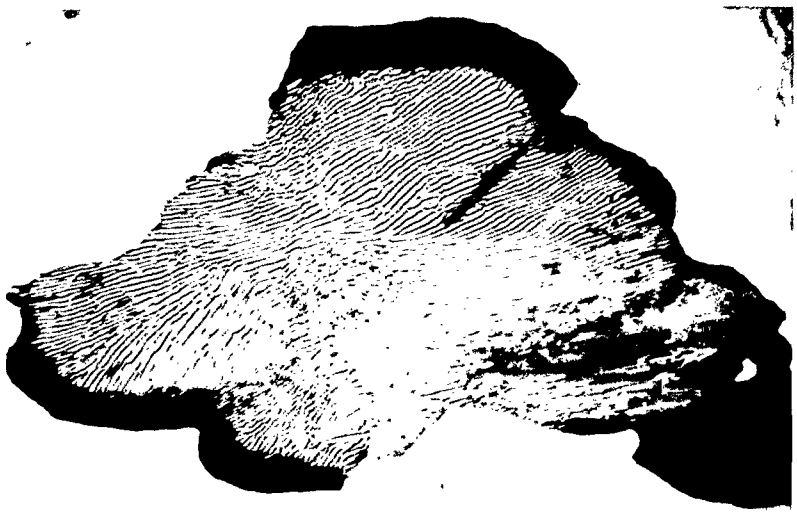

Fig. 22 Run 41. Alloy X transformed for 12 min at 680°C at atmospheric pressure. Note band of finely spaced pearlite formed during quench. Nital etch. 1200X

where V_V is the volume fraction of pearlite transformed at time t, and b and n are temperature-dependent parameters. An indication of the type of nucleation is given by the parameter n. For n = 3 or less, nucleation is sufficiently rapid in comparison with the growth to saturate all the active nucleation sites. For n greater than 4 the nucleation rate is too slow for site saturation and the rate is also increasing with time. Equation (1) can be rewritten as

$$\log \ln (1 - V_V)^{-1} = n \log t + \log b . \qquad (2)$$

Consequently, n can be estimated from the slope of a plot of log ln $(1 - V_V)^{-1}$ vs log t. Such plots for the data listed in Table II are given in Fig. 23. The error bars correspond to the standard deviations of the volume-fraction analyses. The very large values of the initial slope at the three temperatures indicate that nucleation-site saturation had not occurred and that the nucleation rate was time dependent.

Pearlite Interlamellar Spacing

With one exception, the spacing measurements were made on electron micrographs of fully transformed specimens. Samples were electropolished with a "Disa-Electropol" using electrolyte "AC-1." After etching with one per cent nital, carbon replicas were taken which were shadow-cast with platinum at an angle of 30° to the surface. Measurements on the 620°C specimen transformed at 30 kb were made directly under the optical microscope because of the very coarse pearlite spacing in this specimen.

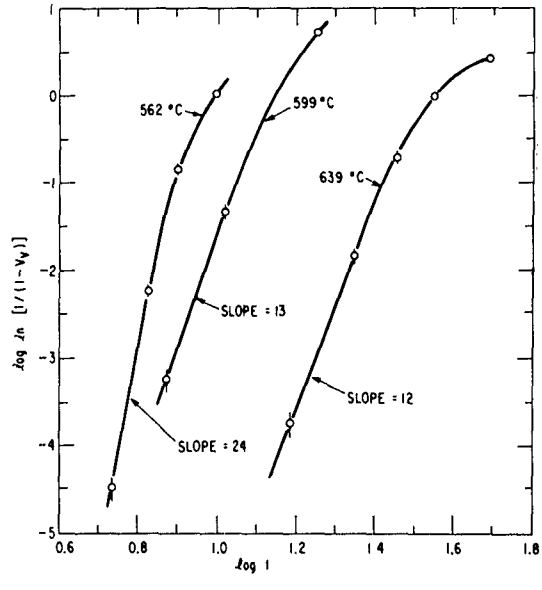

Fig. 23 Plot of log ln $(1 - V_V)^{-1}$ vs log t (where V_V is the volume fraction of pearlite at time t) for alloy X transformed at 562°, 599°, and 639°C at atmospheric pressure.

Micrographs of the four specimens transformed at atmospheric pressure are given in Figs. 24 to 27 and those for the seven specimens transformed at 30 kb are given in Figs. 28 to 34. It will be noted that the pearlite in the atmospheric-pressure specimens retained its characteristic form down to the lowest temperature tested. This was in contrast to the behavior at 30 kb. As shown by the sequence of micrographs in Figs. 28 to 34, the pearlite rapidly becomes degenerate with decreasing temperature. However, a comparison of the highly perfect plate structure found at 600°C and above to the structure at 400°C where only a vestige of the plates remained indicates there was no abrupt transition with temperature in the form of the transformation product.

For the analysis of the spacing, ten exposures were made at randomly selected fields on each replica. A set of 8 x 10-inch prints was then prepared at a magnification of 10,000X, the latter being accurately determined by calibration with a replica of a diffraction grating of known spacing. The three-dimensional property directly estimated was the area of the ferrite-cementite interface per unit volume as given by an intercept analysis. It has been shown[12] that such an analysis is optimized by using a test line in the form of a circle. This automatically yields for each application of the test circle an intercept density which is uniformly averaged over all orientations in the plane of polish. Under these conditions the standard deviation of the analysis is minimized for a given amount of effort.

A test circle of 25 cm circumference printed on transparent plastic was applied at four nonoverlapping positions on each micrograph giving a total of 40 applications per specimen. From a count of the number of intersections of the test circle with ferrite-cementite boundaries in the pearlite, the total boundary area S_V per unit volume was obtained from the relation[12, 13]

$$S_V = 2 N_L \quad , \tag{3}$$

where N_L is the number of boundary intersections per unit length of test line. We can define an average spacing $\bar{s}$ as being the constant spacing that would give the same boundary area per unit volume as that actually present in a given specimen. Since a plate has two faces, it is evident that

$$\bar{s} = 2/S_V \quad , \tag{4}$$

and hence, by Eq. (3),

$$\bar{s} = 1/N_L . \tag{5}$$

The average spacing defined by Eq. (4) is a physically meaningful one because one of the factors that determines the interlamellar spacing of the pearlite is the energy absorbed in the formation of ferrite-cementite boundaries, and this energy is, of course, directly proportional to the total boundary area.

(Copy continued on page 29)

Fig. 24 Electron micrograph of alloy X transformed at 562°C at atmospheric pressure. Nital etch. 10,000X

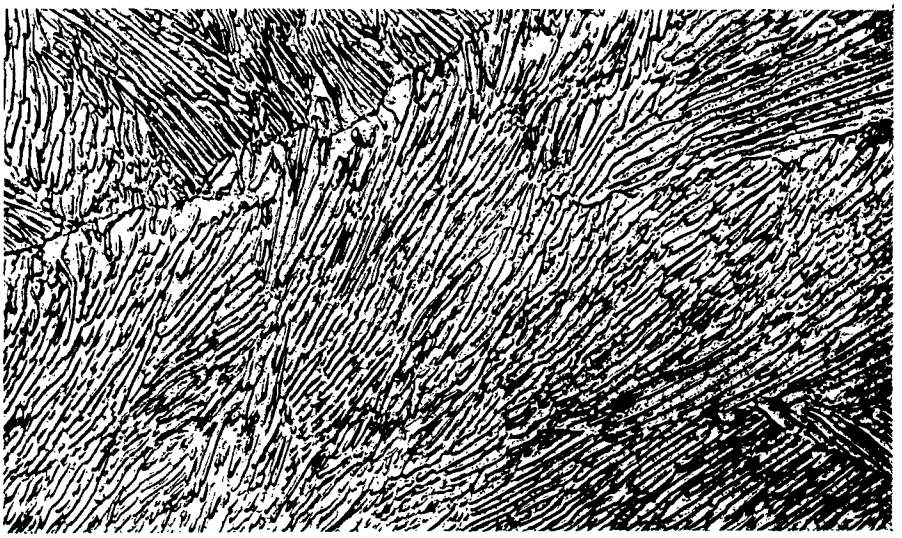

Fig. 25 Electron micrograph of alloy X transformed at 599°C at atmospheric pressure. Nital etch. 10,000X

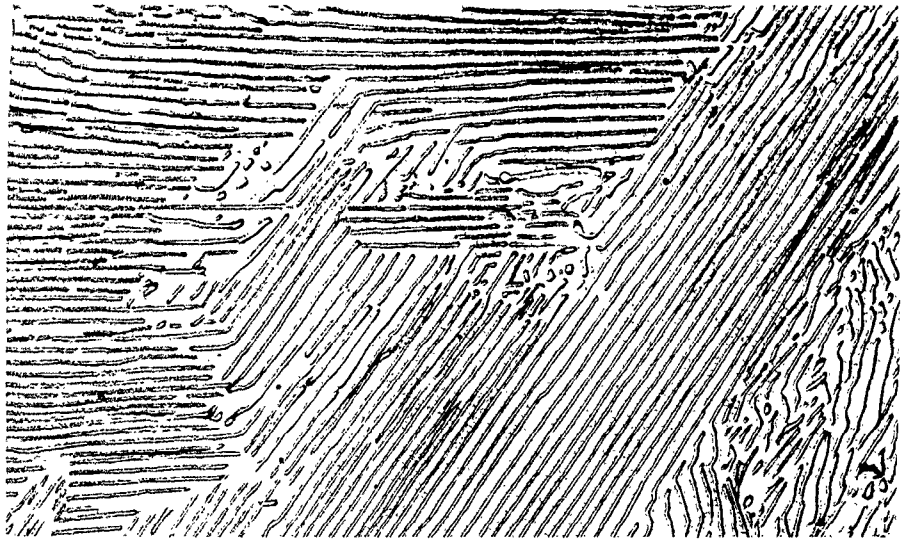

Fig. 26 Electron micrograph of alloy X transformed at 639°C at atmospheric pressure. Nital etch. 10,000X

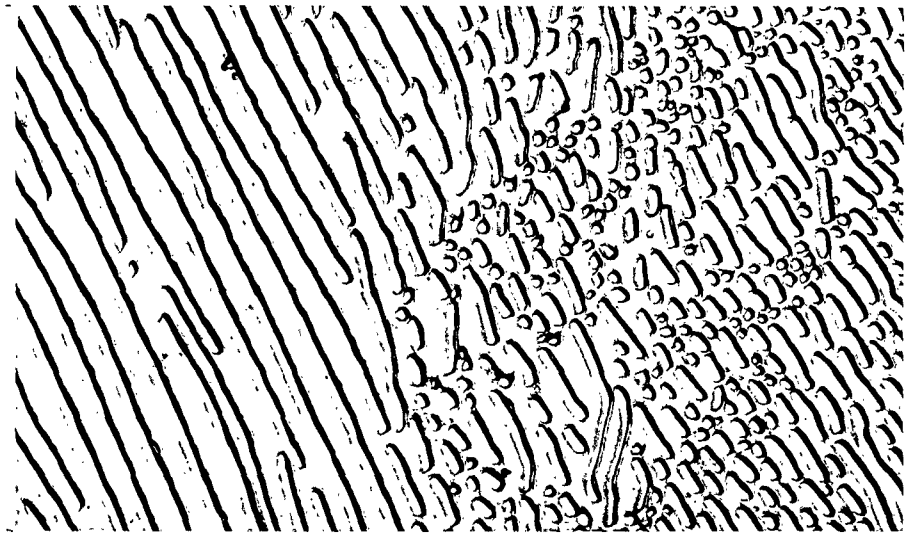

Fig. 27 Electron micrograph of alloy X transformed at 680°C at atmospheric pressure. Nital etch. 10,000X

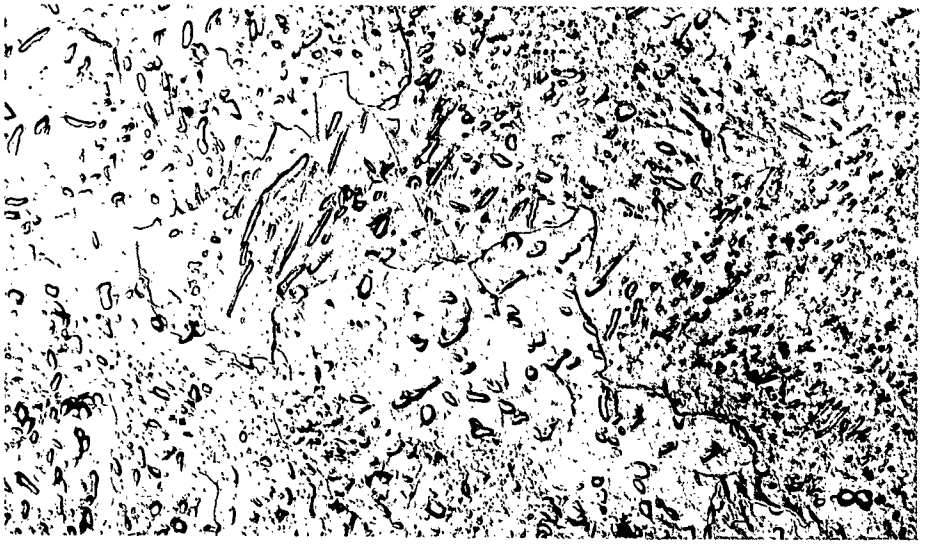

Fig. 28 Electron micrograph of alloy W transformed at 400°C at 30 kb. Nital etch. 10,000X

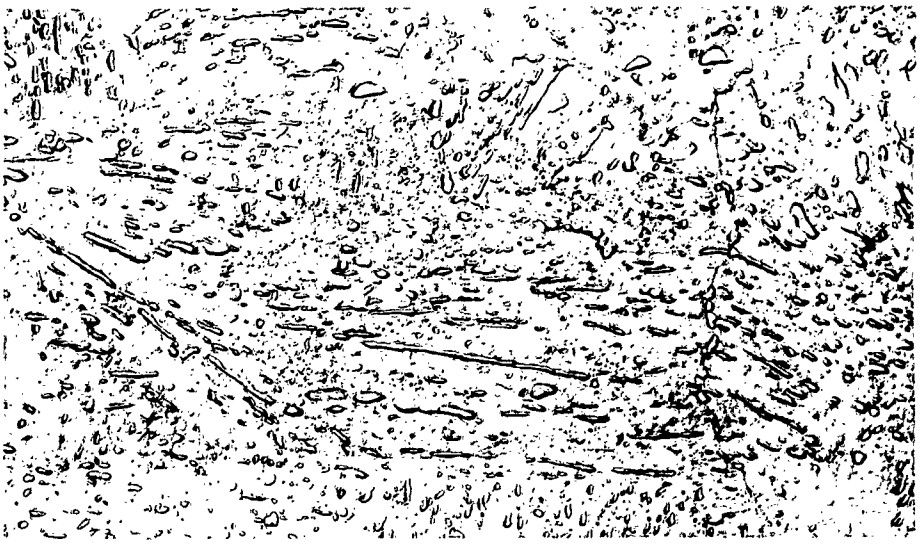

Fig. 29 Electron micrograph of alloy W transformed at 440°C at 30 kb. Nital etch. 10,000X

Fig. 30 Electron micrograph of alloy W transformed at 478°C at 30 kb. Nital etch. 10,000X

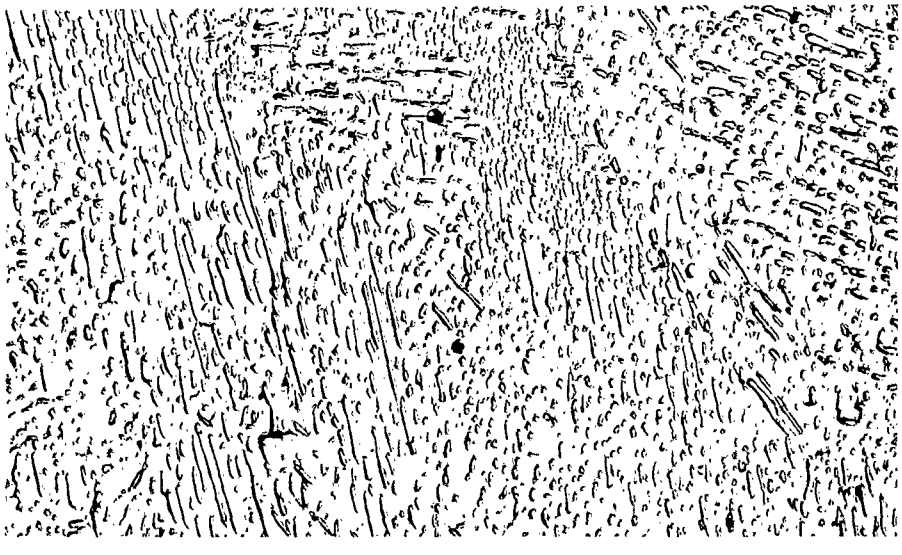

Fig. 31 Electron micrograph of alloy W transformed at 520°C at 30 kb. Nital etch. 10,000X

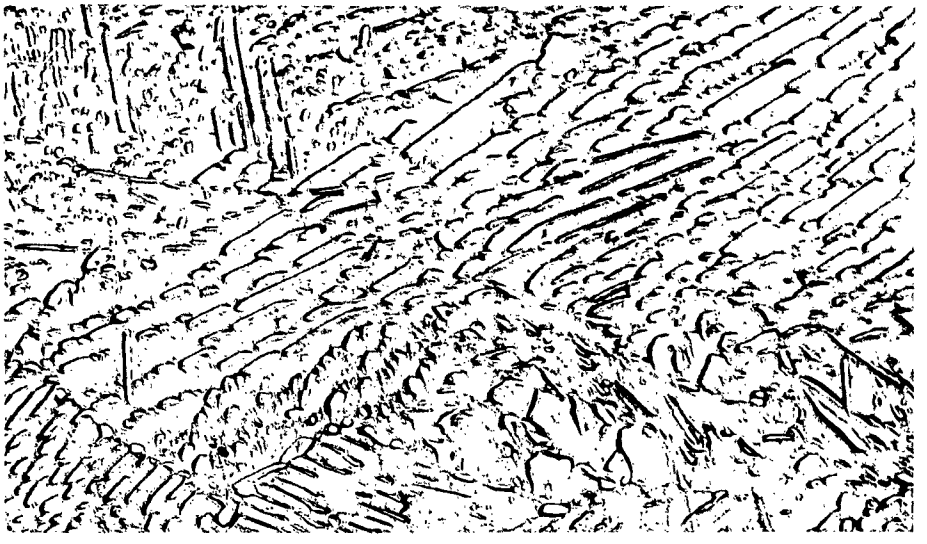

Fig. 32 Electron micrograph of alloy W transformed at 560°C at 30 kb. Nital etch. 10,000X

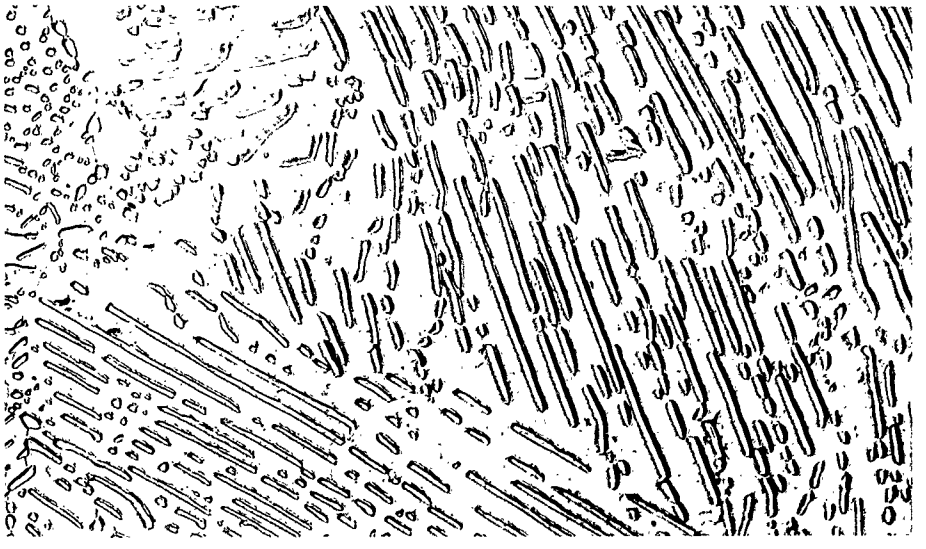

Fig. 33 Electron micrograph of alloy W transformed at 600°C at 30 kb. Nital etch. 10,000X

Fig. 34 Optical micrograph of alloy W transformed at 620°C at 30 kb. Nital etch. 1200X

TABLE VI

Average Interlamellar Spacing*

Alloy	Temperature (°C)	Pressure (kb)	Average Spacing (10^5 A)
X	563	0	1.19±0.04
↓	599	0	1.37± .05
↓	640	0	1.73± .06
↓	680	0	3.6 ± .2
W	400	30	3.9 ±0.1
↓	440	↓	4.0 ± .1
↓	478	↓	4.8 ± .1
↓	520	↓	4.0 ± .2
↓	560	↓	3.4 ± .2
↓	600	↓	3.6 ± .1
↓	620	↓	7.9 ± .4

*"Average spacing" is the constant spacing that would have the same area of ferrite-cementite boundary per unit volume as was actually present in the specimen.

Values for the average interlamellar spacing for specimens transformed both at atmospheric pressure and 30 kb are listed as a function of temperature in Table VI. The observed standard deviations of the measurements are also included. (Because the average spacing $\bar{s}$ is calculated by taking the reciprocal of the measured quantity N_L, the reported values are subject to a small statistical bias. However, this is negligible in comparison with the standard deviations of the measurements.) There are theoretical reasons[11] for believing that the interlamellar spacing should be proportional to the reciprocal of the undercooling below the equilibrium eutectoid temperature. In alloy steels the eutectoid transformation takes place over a range of temperature and there is thus an ambiguity as to what value should be assigned to the "equilibrium" temperature when testing for the reciprocal relationship. This difficulty can be overcome[11] by adopting the simple expedient of plotting the reciprocal spacing against temperature. Such plots for the data given in Table VI are shown in Fig. 35. For the specimens transformed at atmospheric pressure the average spacing decreased monotonically with decreasing temperature, as was to be expected. The disposition of the experimental points and the requirement that zero in reciprocal spacing should fall in the approximate vicinity of the eutectoid temperature (the lower limit of which is 709°C for alloy X according to Picklesimer et al.[4] suggest that, as shown, there should be a change in the slope of the curve at about 640°C. Such a discontinuity was not unexpected, since Picklesimer et al.[4] found that 640°C was the temperature at which partitioning of manganese between ferrite and cementite started to occur. Below this temperature partitioning of the manganese to the cementite did not take place. However, before the discontinuity in slope of the reciprocal spacing vs temperature curve can be considered as having been unequivocally established, it will be necessary to supplement the data shown in Fig. 35 by additional measurements.

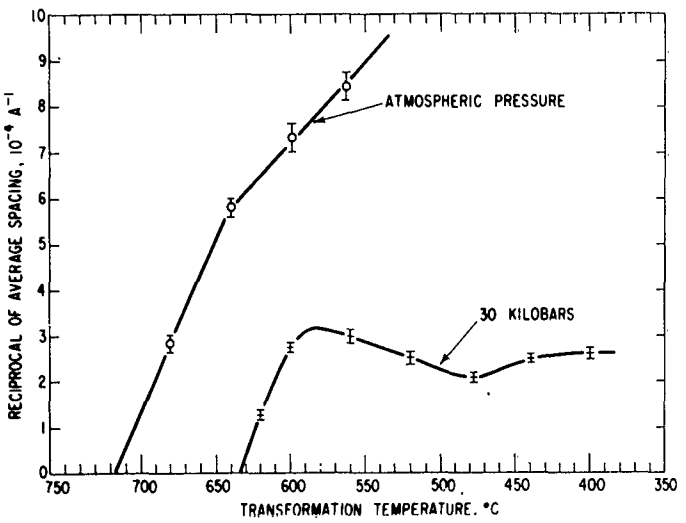

Fig. 35 Reciprocal of the average interlamellar spacing of pearlite vs temperature for alloy X transformed at atmospheric pressure and alloy W transformed at 30 kb.

For the specimens transformed at 30 kb the initial increase in reciprocal spacing with decreasing temperature paralleled the high-temperature branch of the atmospheric-pressure curve. However, this similarity in behavior did not persist to lower temperatures. The 30 kb data displayed a maximum at about 580°C, and thereafter the spacing remained approximately constant. (Perhaps, in view of the extreme degeneracy of the pearlite at 30 kb when formed at low temperatures, it would be more appropriate to claim constancy of cementite boundary area rather than spacing.) It would be interesting to know whether the maximum in the 30 kb reciprocal spacing curve at 580°C corresponded to the onset of manganese partitioning to the cementite. However, no information on this point was obtained during the present investigation.

Austenitic Grain Size

Advantage was taken of the samples prepared for the growth-rate studies to determine the effect of austenitizing under pressure on the austenitic grain size. Analyses were made on randomly selected specimens from the following groups: (a) alloy X austenitized for 10 minutes at 1050°C at atmospheric pressure; (b) alloy W given the same thermal treatment at 30 kb; (c) alloy W austenitized at atmospheric pressure. The last group was included in order to check the effect of carbon content on grain size.

The average austenite grain-boundary area per unit volume was determined for each of the three groups by an intercept analysis performed directly under the microscope. The average boundary area was then converted to an ASTM grain size. This conversion[14] was performed, in effect, by calculating what grain size would be given by a conventional ASTM measurement if it were performed on an imaginary specimen composed of constant-size tetrakaidecahedral grains having the same total boundary area as the specimen under test. Estimates of the standard deviations of the intercept counts were made and converted into the corresponding standard deviations in grain size. The results are listed in Table VII. It will be seen that neither pressure nor carbon content affected the austenitic grain size within the accuracy of the measurements.

TABLE VII

Average Austenitic Grain Size vs Pressure for Alloys Austenitized for 10 Minutes at 1050°C

Alloy	Composition		ASTM Grain Size	
	C (%)	Mn (%)	Atmospheric Pressure	30 kb
W	0.33	1.00	3.8 ± 0.1	3.6 ± 0.1
X	.73	0.97	$3.6 \pm .1$	-

CONCLUSIONS AND SUMMARY

The results of the present investigation have borne out the earlier observations[1, 2] that the application of pressure greatly reduces the growth rate and increases the interlamellar spacing of pearlite in an iron-carbon-manganese alloy. A feature of the transformation not previously detected was the very strong preference for surface nucleation exhibited by the specimens transformed under pressure. Surface nucleation predominated over the whole temperature range studied (440° to 620°C) and, at the higher temperatures, no nodules had nucleated in the interior even after transformation times had allowed considerable growth to occur from the surface. It has not yet been established whether this enhancement of surface nucleation was an intrinsic effect of pressure or whether, instead, it was due to other conditions in the high-pressure cell.

The effect of pressure on the pearlite growth rate is conveniently summarized by Fig. 36, which provides a comparison between the growth rate vs temperature curve at one atmosphere (from Fig. 10) with the curve for specimens transformed at 30 kb. The latter curve is the one for maximum growth rate of surface-nucleated pearlite (as shown in Fig. 19); the average surface growth rate and the maximum nodule growth rate were both smaller by about a factor of two at mid-temperatures and a factor of four at 440°C. A difference in growth rates between the surface and nodular pearlite had not been observed at atmospheric pressure.[4] The high-temperature portions of the atmospheric-pressure and 30 kb growth curves shown in Fig. 36 are displaced from one another by about 90°C, which is roughly the magnitude of the 72°C depression found[1] in the eutectoid temperature of iron-carbon alloys at 30 kb (Fig. 1). However, the 30 kb curve turns over more rapidly with decreasing temperature with the result that the nose (where the growth rate is a maximum) occurs at 560°C--only 20°C below the nose of the atmospheric-pressure growth-rate curve. Thereafter the growth rate at 30 kb falls off less rapidly with decreasing temperature than does the rate at one atmosphere.

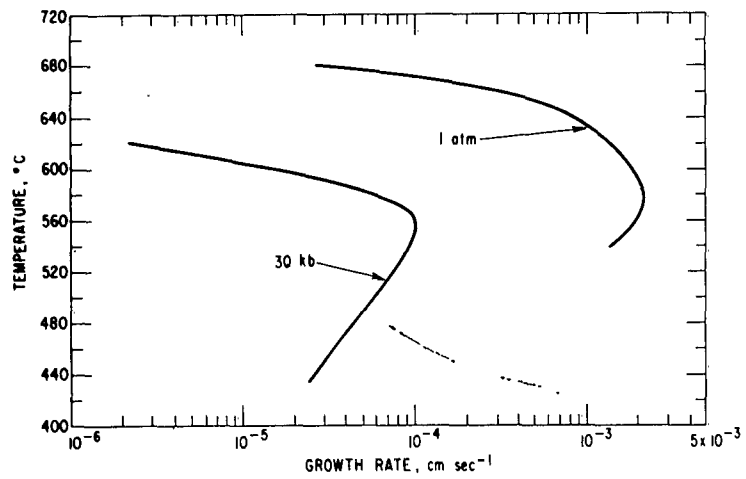

Fig. 36 Pearlite growth rate vs temperature at atmospheric pressure and 30 kb. The 30 kb curve is the one for maximum rate of surface-nucleated growth (cf. Fig. 19).

There were fairly clear indications that at least in the specimens transformed under pressure, the pearlite growth rate was time-dependent; there being a decrease in rate as the transformation proceeded. To the extent that this was true, the growth rates measured in this investigation must be regarded as average values.

For any given transformation temperature there was an appreciable increase with pressure in the interlamellar spacing of the pearlite. However, in terms of undercooling below the equilibrium eutectoid temperature the spacing (like the growth rate) was approximately independent of pressure up to undercoolings of about 50°C. At larger undercoolings this correspondence was lost; the spacing of the atmospheric-pressure pearlite continued to decrease whereas the average spacing (as defined by the ferrite-cementite boundary area) in the 30 kb specimens remained approximately constant or, if anything, actually increased with decreasing temperature. Although the variation with temperature of the atmospheric-pressure spacing was less surprising, the plot of reciprocal spacing (Fig. 35) did display an apparent change in slope at about 640°C. If additional measurements confirm this observation, it will constitute the first experimental evidence for the effect of manganese partitioning on spacing.

Electron microscopy revealed no discontinuous change with temperature in the structure of the pearlite at 30 kb, but extreme degeneracy was observed at the lower transformation temperatures. Finally, austenitization under pressure resulted in no significant change in austenitic grain size within the standard deviation (0.1 ASTM unit) of the measurement.

REFERENCES

1. E.W. Goliber, K.H. McKee, J.S. Kasper, J.E. Hilliard, and V.A. Phillips, "Research and Development on the Effects of High Pressure and Temperature on Various Elements and Binary Alloys," WADC Technical Report 59-747 (March 1960).
2. J.E. Hilliard and J.W. Cahn, "The Effect of High Pressures on Transformation Rates," Progress in Very High Pressure Research, John Wiley and Sons, Inc., New York (1961).
3. J.E. Hilliard and W.R. Tully, "Research and Development on the Effects of High Pressure and Temperature on Various Elements and Binary Alloys," ASD Technical Report 61-21, Part I (May 1961).
4. M.L. Picklesimer, D.L. McElroy, T.M. Kegley, E.E. Stansbury, and J.H. Frye, "Effect of Manganese on the Austenite-Pearlite Transformation," Trans. Met. Soc. AIME, 218, 473 (1960).
5. H.T. Hall, "Ultra-High-Pressure, High-Temperature Apparatus: the 'Belt'," Rev. Sci. Instr., 31, 125 (1960).
6. J.E. Hilliard, J.M. Lommel, J.B. Hudson, D.F. Stein, and J.D. Livingston, "Effect of Annealing under High Pressures on Dislocations in Lithium Fluoride, Aluminum, Copper, and Iron," Acta Met., 9, 787 (1961).
7. F.P. Bundy, "Effect of Pressure on EMF of Thermocouples," Progress in Very High Pressure Research, John Wiley and Sons, Inc., New York (1961).
8. F.P. Bundy, "Calibration Techniques in Ultra-High Pressure Apparatus," Paper No. 60-WA-178, ASME Meeting (November 1960).
9. J.E. Hilliard and J.W. Cahn, "An Evaluation of Procedures in Quantitative Metallography for Volume-Fraction Analysis," Trans. Met. Soc. AIME, 221, 344 (1961).
10. J.E. Hilliard, "Volume-Fraction Analysis by Quantitative Metallography," General Electric Research Lab. Rept. No. 61-RL-2652M (March 1961), to be published.
11. J.W. Cahn and W.C. Hagel, "Theory of the Pearlite Reaction," AIME Symp. on Austenite Decomposition (November 1960); General Electric Research Lab. Rept. No. 60-RL-2582M (December 1960).
12. J.E. Hilliard, "Specification and Measurement of Structural Anisotropy," General Electric Research Lab. Rept. No. 62-RL-2979M (March 1962).
13. C.S. Smith and L. Guttman, "Measurements of Internal Boundaries in Three-Dimensional Structures by Random Sectioning," Trans. Met. Soc. AIME, 197, 81 (1953).
14. J.E. Hilliard (to be published).

Aeronautical Systems Division, Dir/Materials and Processes, Metals and Ceramics Laboratory, Wright-Patterson AFB, Ohio.
Rpt Nr ASD-TDR-62-479, Pt I. RESEARCH ON THE EFFECTS OF HIGH PRESSURE AND TEMPERATURE ON VARIOUS ELEMENTS AND BINARY ALLOYS. Interim report, May 62, 33p. incl illus., tables, 14 refs.

Unclassified Report

The growth rate and interlamellar spacing of pearlite have been determined as a function of transformation temperature at one atmosphere and 30 kilobars pressure in eutectoid iron-carbon alloys containing approximately one percent manganese. The atmospheric-pressure growth rates, measured at four temperatures in the range 560° - 680°C, were in fair agreement with data obtained on a similar alloy by other investigators. Indications were found of a

(over)

change in slope of the reciprocal spacing versus temperature curve at one atmosphere corresponding to the onset of partitioning of manganese between ferrite and cementite at 640°C.

High-pressure runs were made at seven temperatures in the range 400° to 620°C. The most dramatic effect of pressure was a large increase in hardenability - there being up to a thousand-fold reduction in pearlite growth rate.

The results for the effect of pressure on a pearlite growth rate and spacing confirm those obtained at a single temperature in a preliminary survey made earlier in this laboratory.

1. High pressure research
2. High temperature research
3. Binary alloys

I. AFSC Project 7351, Task 735103
II. Contract AF 33(616)-8206
III. General Electric Co., Schenectady, New York
IV. J. E. Hilliard
V. Aval fr OTS
VI. In ASTIA collection

Aeronautical Systems Division, Dir/Materials and Processes, Metals and Ceramics Laboratory, Wright-Patterson AFB, Ohio.
Rpt Nr ASD-TDR-62-479, Pt I. RESEARCH ON THE EFFECTS OF HIGH PRESSURE AND TEMPERATURE ON VARIOUS ELEMENTS AND BINARY ALLOYS. Interim report, May 62, 33p. incl illus., tables, 14 refs.

Unclassified Report

The growth rate and interlamellar spacing of pearlite have been determined as a function of transformation temperature at one atmosphere and 30 kilobars pressure in eutectoid iron-carbon alloys containing approximately one percent manganese. The atmospheric-pressure growth rates, measured at four temperatures in the range 560° - 680°C, were in fair agreement with data obtained on a similar alloy by other investigators. Indications were found of a

(over)

change in slope of the reciprocal spacing versus temperature curve at one atmosphere corresponding to the onset of partitioning of manganese between ferrite and cementite at 640°C.

High-pressure runs were made at seven temperatures in the range 400° to 620°C. The most dramatic effect of pressure was a large increase in hardenability - there being up to a thousand-fold reduction in pearlite growth rate.

The results for the effect of pressure on a pearlite growth rate and spacing confirm those obtained at a single temperature in a preliminary survey made earlier in this laboratory.

1. High pressure research
2. High temperature research
3. Binary alloys

I. AFSC Project 7351, Task 735103
II. Contract AF 33(616)-8206
III. General Electric Co., Schenectady, New York
IV. J. E. Hilliard
V. Aval fr OTS
VI. In ASTIA collection